AD-A081 563 IOWA UNIV IOWA CITY DEPT OF CHEMISTRY F/G 7/4
MICROSCOPIC RATE CONSTANTS FOR D + F2,(U)
1979 D C TARDY, S BITTENSON, J WANNA N00014-78-C-0577
UNCLASSIFIED NL

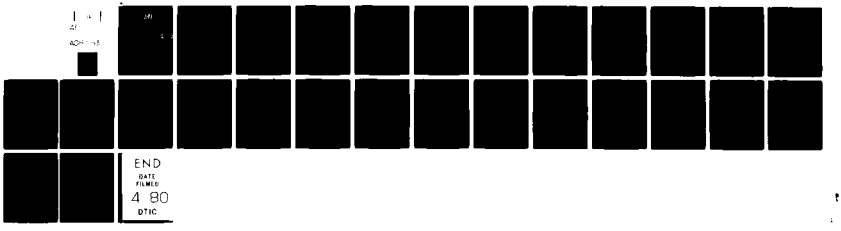

END
DATE FILMED
4 80
DTIC

LEVEL II

12

MICROSCOPIC RATE CONSTANTS FOR D + F_2

10 D. C. Tardy* S. Bittenson J. Wanna
Department of Chemistry
The University of Iowa
Iowa City, Iowa 52242

12 09

*Principal Investigator

Prepared for Office of Naval Research
Under Contract N00014-78-C-0577
11 1979
15

79-12 27 020

15842

INTRODUCTION

The vibrational energy distributions resulting from exoergic bimolecular exchange reactions of the type: $A + BC \longrightarrow AB + C$ have been successfully determined by the Chemiluminescence Techniques pioneered by Polanyi and co-workers.[1] Specifically, nascent population distributions have been obtained using the Arrested Relaxation (AR) method[2-5] in which the reaction takes place in a low pressure (< 1 micron), cold wall, fast pumping speed environment. These conditions are required so that

i. gas phase collisions resulting in vibrational energy transfer are reduced

ii. wall collisions will completely deactivate the energy rich product molecules

iii. multiple emission is negligible.

A block diagram depicting the traditional AR apparatus is shown in Figure 1.

Although the AR method has produced valuable information pertaining to energy distributions, the following modifications would be highly desirable so that 'undoable' reactions could be performed:

(1) increase the atom concentration by effectively increasing the dissociation efficiency of the atomic precursor without the addition of an inert gas (the location of the microwave cavity is undesirably far from the orifice decreasing the effective molecular dissociation);

(2) decrease reagent throughput so that reasonable pumping systems can be used;

(3) eliminate wavelength dependence of baseline (the lock in amplifier derives its output from the difference in emission between the chopper blade (thermal) and the reaction vessel (thermal + chemiluminescence) so that the zero reaction signal depends on wavelength);

next page

cont

(4) observe time evolution of the product distribution so that relaxation and secondary processes can be deconvoluted;

(5) increase S/N by signal averaging; and

(6) introduce data storage so that more efficient processing can be used.

For the DF2 system (the prime reaction of this report)

$$D + F_2 \rightarrow DF(v) + F \qquad \Delta E_o^\circ = 100 \text{ kcal/mole} \qquad (1)$$

vibrational levels up to v = 15 can be populated. Scanning the 3.0 to 5.5 micron region is necessary if the fundamental emission is monitored. The large number of emission lines in this region make automated data acquisition/processing a real necessity. This wavelength range also produces a large baseline drift so that a detecting system with a large dynamic range and the capability of easily converting the raw data to that originating solely from the chemiluminescence is needed. Another problem associated with this system is that the D atom recombination (or the inefficiency in producing D) produces D_2 so that the secondary reaction

$$F + D_2 \rightarrow DF + D \qquad v(max) = 4 \qquad (2)$$

can occur. The importance of this process is enhanced by the fact that k(2) is approximately 8 times faster than k(1) {$k(2) = 1.3 \times 10^{13} cm^3 mol^{-1} sec^{-1}$ (ref. 6)}.

Polanyi and Sloan[4] (PS) have reported the energy distribution for the $H + F_2$ (HF2) system as is summarized in Table 1 and Figure 2. Their experiments used very large reagent flows (~500 μmoles/sec of F and ~ 200 μmoles/sec of argon (the argon was used to increase the H atom yield); to maintain a low pressure (0.3 microns) cryogenic (30°K) pumping was used.

For AR experiments producing HF the radiative relaxation rate is comparable to the pump out rate: the effect of this perturbation on the

observed steady state population distribution was evaluated by model calculations. The details of these steady state calculations, for which collisional relaxation was ignored are presented in the Appendix. A summary plot of these results for the HF2 system are shown in Figure 3. The observed distribution undergoes a dramatic change as the pumping rate changes from 10^4 to 10^3 sec^{-1}. PS estimate that the pumping rate for their system is approximately 500 sec^{-1}. Thus these calculations indicate that the distribution observed in the PS experiment may be partially relaxed: the nascent distribution may peak at v = 7. In determining the effect of reagent energy on distribution for the HF_2 system Polanyi and co-workers[5] obtained a distribution peaking at v = 5 in a non-cryogenically pumped reaction vessel. This was attributed to the dynamics; these calculations indicate that radiative relaxation could indeed generate this observation.

The importance of other experimental parameters (reagent flow, percent dissociation, background pressure, etc.) was evaluated by integrating the appropriate rate equations. A summary of these calculations are shown in Table 2 while the details are presented in the Appendix. The important points are that both high percentage dissociation and a high flow of fluorine in a fast pumping system are required for the AB experiments.

CHEMILUMINESCENT MAPPING

It is clear from these calculations that in order to perform the DF2 experiments (smaller rate constant and smaller emission rates) the traditional AR experiments will not work. Thus a new Chemiluminescent method, herein called "Chemiluminescent Mapping" (i.e. CM) had to be developed. The essence of CM is that a pulsed technique is used so that lower flows can be used and that the time dependence of the full emission spectra is measured so that secondary processes (reaction and radiative and collisional

relaxation) can be determined. The apparatus for performing a CM experiment is shown in Figure 4.

The CM system is based around a microcomputer which provides: i) controls for synchronizing a six channel gated integrator, ii) pulses for the fluorine chopper (a closeup of the chopper is shown in Figure 5), iii) pulses to the stepper motor on the monochromator, iv) A/D and D/A conversion, v) data storage. The F_2 chopper provides 100% modulation of the reaction so that with a typical 10% duty cycle the F_2 flow is reduced by a factor of 10 over the AR experiments. This in turn puts a smaller load on the pumping system. Of equal importance is that the baseline drift is eliminated. A new microwave cavity was designed to maximize the D atom production rate by allowing the discharge to be adjacent to the reaction site (see Figure 5). The cavity is cooled by cold nitrogen gas and does not have any sliding vacuum seals.

In a typical experiment the wavelength is scanned at a speed commensurate with the required S/N. At each grating step, a predetermined number (N) of chopper (reaction) pulses are made. (The intensity profile for a reaction pulse is shown in Figure 6.) The time between chopper pulses is determined by the intensity-time profile: under normal conditions this corresponds to approximately 100 milliseconds. Similarly the positions of six sampling windows of the emission intensity are decided. These windows are integrated over the window width (~ 5 msec) and then summed over the N pulses. After stepping through the whole spectral region the complete emission profile for the 6 time windows is stored. Five 'real' spectra are obtained by subtracting the reference channel (the window before each chopper pulse) from the other channels. The intensities are then corrected for detector (InSb) response and instrumentation transmission by comparison with a Blackbody Radiation source. These "equal response" intensities are then related to the populations by the Einstein Coefficients published by Meredith and Smith.[7]

From the observed time and pressure dependences the contributions due to radiative and collisional relaxation and secondary reaction (if present) can be evaluated.

CONFIRMATION OF THE CM TECHNIQUE

To test and evaluate the CM technique the vibrational energy distribution for the reactions

$$F + H_2 \rightarrow HF(v) + H$$
$$F + D_2 \rightarrow DF(v) + D$$

were measured. The available energies of 34.6 and 34.7 kcal/mole,[8] respectively are calculated from the zero point energy difference of reactants and products, the critical energies for reaction and the thermal energy of the reactants; so v(max) for these reactions are 3 and 4, respectively. The time evolution of specific vibration-rotation levels for HF from the $F+H_2$ reactions is shown in Figure 7. On this semi-log plot the parallel behavior indicates that the main processes are production (chemical reaction) and physical removal (pumping and wall collisions resulting in complete deactivation). The relative population distribution appears to be independent of time. However, the low v, low J (1,1 and 2,1) lines show that relaxation is becoming important between 23 and 28 milliseconds. A summary table of the vibrational populations are presented in Table 3. It is clear that the distributions are indeed within experimental error of those previously reported. Thus we are confident of the validity of the CM results.

DF2 RESULTS

The CM for $D + F_2$ (E(availabe) = 100 kcal/mole, v(max) = 15)) was performed under the following experimental conditions:

background pressure = 1 micron

D_2 flow = 0.84 μmoles/sec

F_2 flow = 43 μmoles/sec

Only vibrational levels from 10 through 13 were detected. The rotational distribution for these levels are shown in Figure 8; a bimodal distribution speaking at J = 1 (thermal) and J = 6 or 7 is observed.

The vibrational distribution is directly compared to what has been reported for the HF2 system as shown in Figure 2. From first principles it is expected that for isotopic variants of a particular reaction that an universal curve will result when the populations are plotted as a function of the fractional energy in vibration (i.e. f_v = E(vib)/E(avail). However, for the DF2 system this is not the case; the most probable population occurs at f(v) = 0.74 contrasted to 0.58 for the HF2 system. Part of this difference may be due to relaxation in the PS experiments. At this time a detailed explanation for this 15 kcal/mole difference can not be given. An important point is that in the DF2 distribution that there is no emission observed from levels with v<10. It is also noteworthy that it is difficult to envision any processes which would push the most probable level upwards; i.e. experimental problems will in general produce relaxation, and peaking at lower levels.

Nevertheless two features of the chemiluminescence from high vibrational levels of DF produced by this reaction indicate that we may be observing optical gain among these levels. The first observation is the non-parallel time evolution of the emission intensity from various rotational states. This is shown in Figure 9 for DF(v = 11). In the absence of any relaxation processes, the plots for these states should be parallel, as in the case for the FH2 reaction (Figure 7). Small deviations from parallelism can be accounted for by the change in the probabilities for spontaneous emission from the states involved. However, these erratic time evolution curves cannot

be explained in this manner and are taken as evidence of optional gain. The second indication of a possible gain situation in this system is a very strong dependence of the signal level upon chopper duty cycle. The relative intensities of various transitions are also very duty cycle dependent. In the current apparatus a pressure threshold for very intense emission exists, (this is demonstrated by detection system saturation). Faster temporal evolution measurements may provide further evidence of gain if such a situation is occurring, such experiments are planned but as of this time have not been performed.

Consider the reaction: $A + BC \xrightarrow{k_{vJ}} AB_{rJ} + C$

where $k_i = k_{vJ}$, rate $_{vJ} = r_i = k_i N_A N_{BC}$

and N_I is the number density of the I^{th} species. A master equation can be written down for each quantum level i (i corresponds to the set of quantum levels: translation, rotation, vibration, electronic, etc.)

$$\frac{dN_i}{dt} = -\tau_i^{-1} N_i + r_i - \omega \Sigma_i p_{ij} N_j + \omega \Sigma_j p_{ij} N_j - \Sigma_i A_{ij} N_j + \Sigma_j A_{ij} N_j \qquad (1)$$

where τ_i is the pumping lifetime of the i^{th} state in the reaction vessel

ω is the collision frequency

P_{ij} is the probability per collision for transfer from j to i

A_{ij} is the rate constant for spontaneous emission (Einstein coefficient) from j to i; $j = i + \Delta$. $\Delta = 1,2,3,$etc.

Equation 1 can be recast into matrix notation

$$\dot{\vec{N}} = -\overleftrightarrow{\tau}^{-1} \vec{N} + \vec{r} + \omega \overleftrightarrow{P} \vec{N} + \overleftrightarrow{\alpha} \vec{N}$$

for $i \neq j$

$\tau_{ij} = 0$

$P_{ij} = P_{ij}$

$\alpha_{ij} = A_{ij}$

for $i = j$

$\tau_{ii} = \tau_i$

$P_{ij} = -1$

$\alpha_{ii} = -\Sigma_{i<j} A_{ij}$

For a steady state $\dot{\vec{N}} = 0$ so $r = \overleftrightarrow{\tau}^{-1} \vec{N}^{ss} - \omega \overleftrightarrow{P} \vec{N}^{ss} - \alpha \vec{N}^{ss}$ (2)

Thus the k_i's (which are proportional to the r_i's can be obtained from the steady state populations, the P_{ij}'s and A_{ij}'s. The N_i's are computed from the emission intensities (E_{ij}^{obs}) for a particular transition $j \rightarrow i$ by

$$N_i \propto \frac{E_{ji}^{obs}}{A_{ji}} \tag{3}$$

For AR, $\tau^{-1} N^{ss} >> \omega P N^{ss} + \alpha N^{ss}$

since a low pressure ($\omega \rightarrow 0$) fast pumping system is used. Assuming

$\tau_i^{-1} = \tau_j^{-1} = \tau^{-1}$ it can be shown that $k_i \propto N_i \propto \frac{E_{ij}^{obs}}{A_{ij}}$

For the model calculations described herein the Einstein coefficients calculated by Meredith and Smith[7] were used (they compare favorably with those experimentally obtained by Sileo and Cool[11]). The rate constants out of a vibrational level due to emission, including various overtone transitions, are given in Figure 10. It should be noted that if only fundamental transitions are included the maximum radiative rate constant appears at v = 5 as contrasted to the real situation where the rate constant monotonically increases. In fact for v = 7 the first overtone is faster than the fundamental. Thus, for correct modeling with experimental data, transitions up to at least $\Delta v = 3$ must be included. This is shown in Table IV where the effect of overtone transitions on the observed populations distribution is exhibited. If these overtone transitions are not included in the modeling, then extrapolation to 'zero' radiative relaxation will produce an "initial" distribution narrower than would appear if a complete calculation had been performed; this is demonstrated in Table IV. Hence, all our calculations include overtone transitions.

The dependence of the observed population distribution on pumping lifetime is portrayed in Table V and Figure 3. It can be seen that as long as τ is less than $\sim 3 \times 10^{-5}$ seconds radiative relaxation is unimportant. However, these calculations also indicate that with $\tau \sim 10^{-4}$ seconds that the observed distribution will be widened by radiative relaxation; lower levels have enhanced populations. In fact with $\tau = 10^{-3}$ seconds, the most probable population occurs at $v = 5$.

To provide insight into the effect of the experimental parameters on the population distribution for the HF2 system, we have also performed model calculations by integrating the set of coupled differential equations in which collisional effects are neglected and secondary reaction ($F + H_2$) is included

$$\dot{\vec{N}} = \vec{r}_1 - \overleftrightarrow{\tau^{-1}} \vec{N} + \overleftrightarrow{\alpha} \vec{N} + \vec{r}_2$$

where

$$r_1 = f_1(c,t)\ k_r(H + F_2)\ N_H\ N_{F_2}$$

$$r_2 = f_2(c,t)\ k_r(F + H_2)\ N_F\ N_{F_2}$$

and $f(c,t)$ is a time dependent reaction configuration function depending on the geometry of the reaction vessels. The emission intensities are calculated as before (equation 3). These calculations take into consideration that the reactants are not collimated so that the molecular density decreases as they approach the pumping part; reaction can take place as long as reactants are contained in the reactor.

In addition to microscopic kinetic information (k_{vj}) and Einstein transition probabilities, modelling parameters include:

flows of reactants

efficiency of atom formation from molecular hydrogen

reaction chamber pressure

reaction dependence on reactor geometry

After integration, the resulting output contains the final pressure of all reactants and products and the fundamental and overtone emission of HF from the primary and secondary reactions. Examples of representative runs are presented in Table II. In essence the spirit of these calculations is to simulate intensity distributions from a given initial distribution for a specific set of experimental parameters.

The intensity distribution for $H+F_2$, $D+F_2$, $F+H_2$ and $F+D_2$ for $\tau = 0$ is shown in calculations 8, 10, 11, and 12, respectively. Comparing calculations 1 and 3 or 2 and 4 or 4 and 5 shows the strong dependence of secondary reaction on H_2 flow and/or % dissociation. The dependence of intensity for the $1 \rightarrow 0$ fundamental transition on flow velocity is also demonstrated; from calculation 1 and 2 an increase in background pressure of a factor of 5 produces a decrease in the velocity of 5. For this minimal increase the intensity increases by 1000 while the $v = 1$ relative population has changed by less than a factor of 2. The PS experiments have been simulated as shown in calculation 6 (we have assumed 90% dissociation); as can be seen the intensity distribution is within experimental error of the $\tau = 0$ calculation (#8). It is important to note that if the background pressure is a factor of two larger that a wider distribution peaking at $v = 5$ (instead of $v = 6$) will be observed (calculation #&). Thus it is very apparent that the results of PS are close to the transition region where the calculated populations may be in error. With out original AR experimental system (steady state, 10% dissociation, with mass flows less than 10^4 cm/~sec) the populations' distributions were highly relaxed as is predicted by these calculations.

The situation is somewhat worse for $D + F_2$ in which there is a higher density of states (more levels to distribute the energy), a smaller rate constant (x0.5) and smaller Einstein coefficients. A simulation for this reaction is shown in calculation 9. These results bear out the reason why results for this reaction have not been reported even though the H reaction had been reported nearly 7 years ago.[4]

REFERENCES

1. a) J. K. Cashion and J. C. Polanyi, J. Chem. Phys., 29, 455 (1958).

   b) P. E. Charters and J. C. Polanyi, Disc. Far. Soc., 33, 107 (1962).

   b) K. G. Analuf, P. J. Kuntz, D. H. Maylotte, P. D. Pacey, and J. C. Polanyi, Disc. Far. Soc., 44, 183 (1967).

2. J. C. Polanyi and K. B. Woodall, J. Chem. Phys., 57, 1574 (1972).

3. D. S. Perry and J. C. Polanyi, Chem. Phys., 12, 419 (1976).

4. J. C. Polanyi and J. J. Sloan, J. Chem. Phys., 57, 4988 (1972).

5. J. C. Polanyi, J. J. Sloan, and J. Wanner, Chem. Phys., 13, 1 (1976).

6. R. Foon and M. Kaufman, "Kinetics of Gaseous Fluorine Reactions," in Progress in Reaction Kinetics, Volume 8, Part 2, Edited by K. R. Jennings and R. B. Cundal, Pergamon Press (1975).

7. R. E. Meredith and F. G. Smith, "Investigations of Fundamental Laser Processes", Volume 2, Willow Run Laboratories, Ann Arbor, Michigan (1971).

8. M. J. Berry, J. Chem. Phys., 59, 6229 (1973).

9. H. W. Chang and D. W. Setser, Chem. Phys., 58, 2298 (1973).

10. J. G. Moehlmann and J. C. McDonald, J. Chem. Phys., 62, 3061 (1975).

Table I

Product Vibrational Population Distributions

Vibrational Level	Arrested Relaxation For $H + F_2$ (Ref. 4)	Chemiluminescence Mapping For $D + F_2$ (This Work)
1	.12	
2	.13	
3	.25	
4	.35	
5	.78	
6	1	
7	.40	
8	.26	
9	<.16	
10		$0.10 \pm .03$
11		1.0
12		$.58 \pm .05$
13		$.29 \pm .05$

Table II

Spectral Intensity Distributions from Model Calculations

(collisional relaxation not included)

Calculation Number	Reaction Conditions: Flows (μ mole/sec) F_2	H_2	Pressure (torr)	% $H_2(D_2)$ Dissociation	Mass Flow (cm/sec)	$\frac{\Sigma HF_{cold}}{\Sigma HF_{hot}}$ [a]	Relative Intensity for 1-0	Fundamental Intensity Distribution for v = 1	2	3	4	5	6	7	8	9	10	11	12
1	50	3.2	2×10^{-4}	10	4.4×10^{4}	.0037	1.8×10^{-5}	.06	.11	.27	.41	.86	1.0	.35	.19				
2	50	3.2	1×10^{-3}	10	8.9×10^{3}	.093	1.5×10^{-2}	.10	.26	.46	.60	.97	1.0	.33	.17				
3	50	32	3×10^{-4}	1	4.4×10^{4}	.039	2.0×10^{-5}	.06	.15	.29	.41	.85	1.0	.35	.18				
4	50	32	1.5×10^{-3}	1	8.9×10^{3}	.59	3.8×10^{-2}	.24	.88	.90	.58	.98	1.0	.34	.17				
5	50	32	2×10^{-3}	90	9.2×10^{3}	.079	1	.09	.25	.44	.58	.98	1.0	.33	.17				
6 [b]	500	3.2	3×10^{-4}	90	5.9×10^{4}	.00005	1×10^{-4}	.06	.11	.26	.40	.85	1.0	.35	.19				
7	500	3.2	5×10^{-3}	90	3.5×10^{3}	.02	2.9	.14	.37	.71	.95	1.16	1.0	.32	.15				
8 [c]	~0	~0	~0	100	free molecular	0		.05	.10	.24	.37	.83	1.0	.35	.19				
9	60	10(D_2)	2×10^{-3}	50	6.2×10^{3}	0.26	2.1×10^{-2}	.04	.14	.31	.38	.46	.64	.83	.94	1.0	.43	.26	.04
10 [d]	~0	~0(D_2)	~0	100	free molecular	0		.03	.07	.16	.25	.40	.55	.72	.88	1.0	.44	.28	.04
11 [c]	~0(F)	~0(H_2)	0		free molecular			.17	1.0	.81									
12 [c]	~0(F)	~0(D_2)	0		free molecular			.10	.42	1.0	.71								

Notes

a. Total HF(DF) produced by F + $H_2(D_2)$/total HF(OF) produced by H(D) + F_2.

b. Conditions for calculation 6 from PS experiments (reference 3).

c. Population distributions for calculations 8, 11 and 12 taken from references 3, 2 and 2, respectively.

d. Population distribution for calculation 10 derived from reference 3 using Surprisal Analyser.

Table III

Observed Vibrational Population Distributions

Vibrational Level	$F + H_2$					
	AR^a	AR^b	AR^c	AR^d	CL^e	CM (Present Work)
1	.31	.28	.31	.28	.29	.27±.07
2	1.0	1.0	1.0	1.0	1.0	1.0
3	.47	.57	.51	.47	.63	.44±.04

	$F + D_2$			
	AR^a	AR^b	CL^e	CM (Present Work)
1	.28	.16	.24	.31±0.10
2	.65	.53	.56	.58±.09
3	1.0	1.0	1.0	1.0
4	.71	.58	.40	.80±.08

a) From Reference 3
b) From Reference 2
c) From Reference 9
d) From Reference 10
e) Chemical Laser Technique From Reference 8

Table IV

Effect of Overtone Transitions on Steady State Populations

Pumping Rate = 2.5×10^3 $sec^{-1} = \tau^{-1}$

Vibrational Level	Initial Distribution[a]	Including Transitions Up To ΔV = 1	2	3	4	5
0	0	.012	.017	.017	.017	.017
1	.13	.16	.18	.19	.19	.19
2	.20	.25	.30	.31	.31	.31
3	.30	.38	.47	.48	.48	.48
4	.51	.62	.72	.73	.73	.73
5	.88	.96	1.02	1.01	1.01	1.0
6	1.0	1.0	1.0	1.0	1.0	1.0
7	.45	.46	.43	.43	.43	.43
8	.28	.27	.25	.25	.25	.25

a) Relative populations obtained from Reference 4.

Table V

Steady State Population Distribution Dependence on "Pumping" Rate

Vibrational Level	Pumping Rate (sec^{-1})							
	[∞	10^5	$3.3x10^4$	10^4	$3.3x10^3$	10^3	$3.3x10^2$	10^2]
0	0	.00029	.00091	.0033	.0012	.081	.82	8.4
1	.13	.13	.13	.14	.17	.35	1.26	4.1
2	.20	.20	.21	.22	.28	.55	1.39	2.9
3	.30	.30	.31	.34	.44	.76	1.45	2.3
4	.51	.52	.53	.57	.68	.98	1.43	1.9
5	.88	.88	.89	.92	.98	1.13	1.31	1.5
6	1.0	1.0	1.0	1.0	1.0	1.0	1.0	1.0
7	.45	.45	.45	.44	.43	.41	.39	.38
8	.28	.28	.28	.27	.25	.23	.20	.18

a) Relative Populations from Reference 4.

Figure 1

CHEMILUMINESCENCE (ARRESTED RELAXATION) EXPERIMENTS

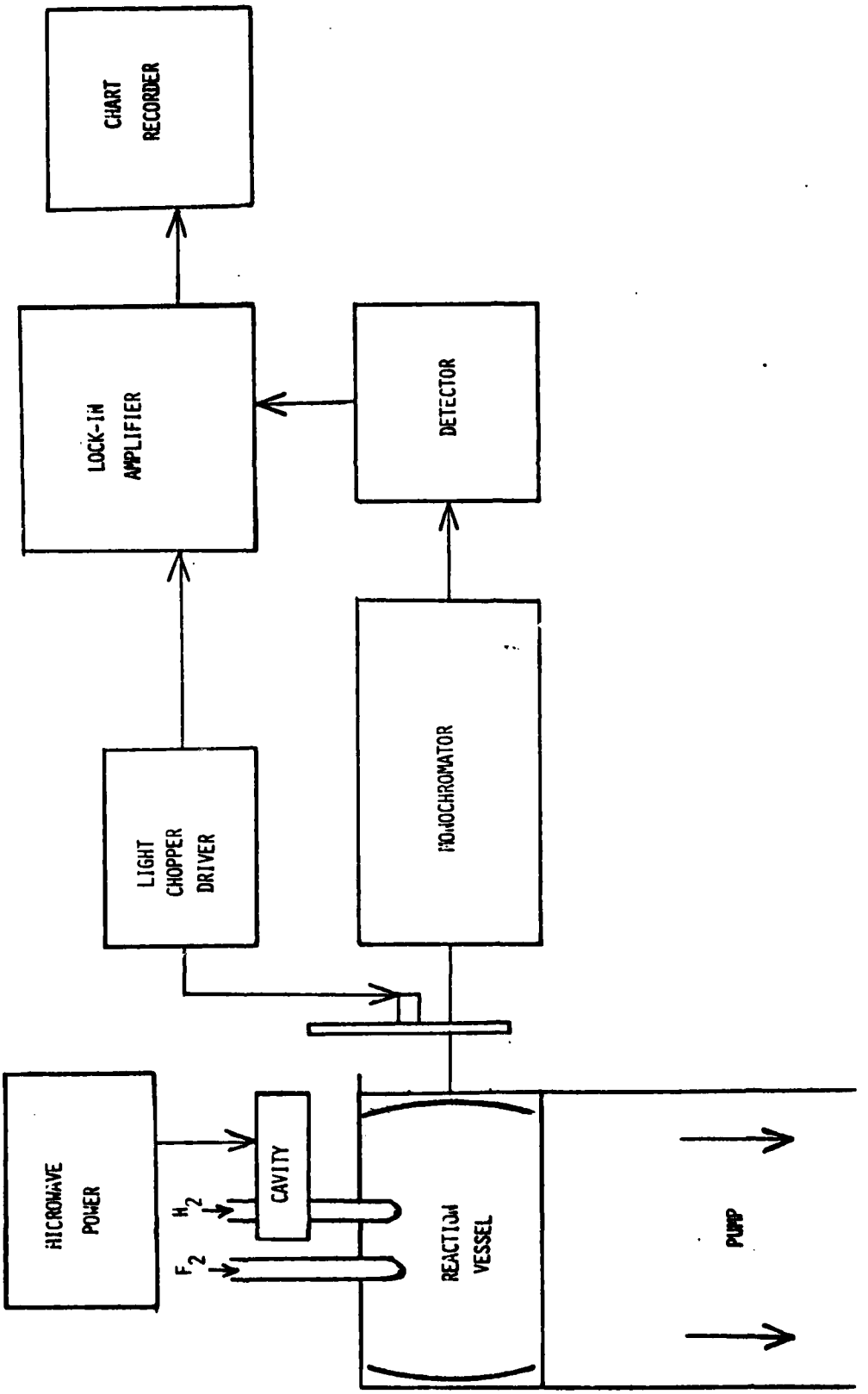

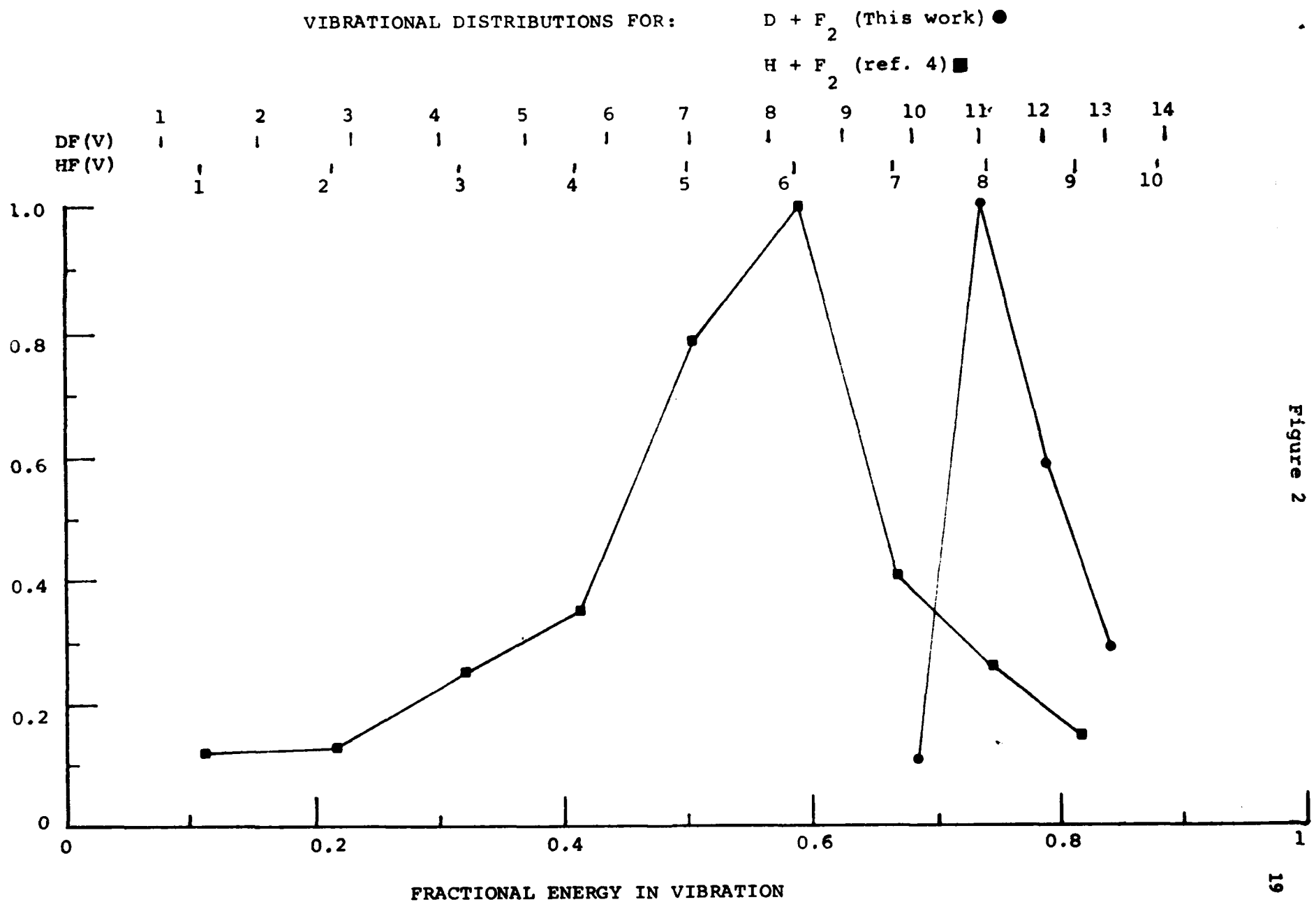
VIBRATIONAL DISTRIBUTIONS FOR:
D + F2 (This work) ●
H + F2 (ref. 4) ■
DF(V)
HF(V)
1.0
0.8
0.6
0.4
0.2
0
0.2
0.4
0.6
0.8
1
FRACTIONAL ENERGY IN VIBRATION

Figure 2

Figure 3

STEADY STATE POPULATION DISTRIBUTIONS FOR VARIOUS PUMPING RATES (γ^{-1})

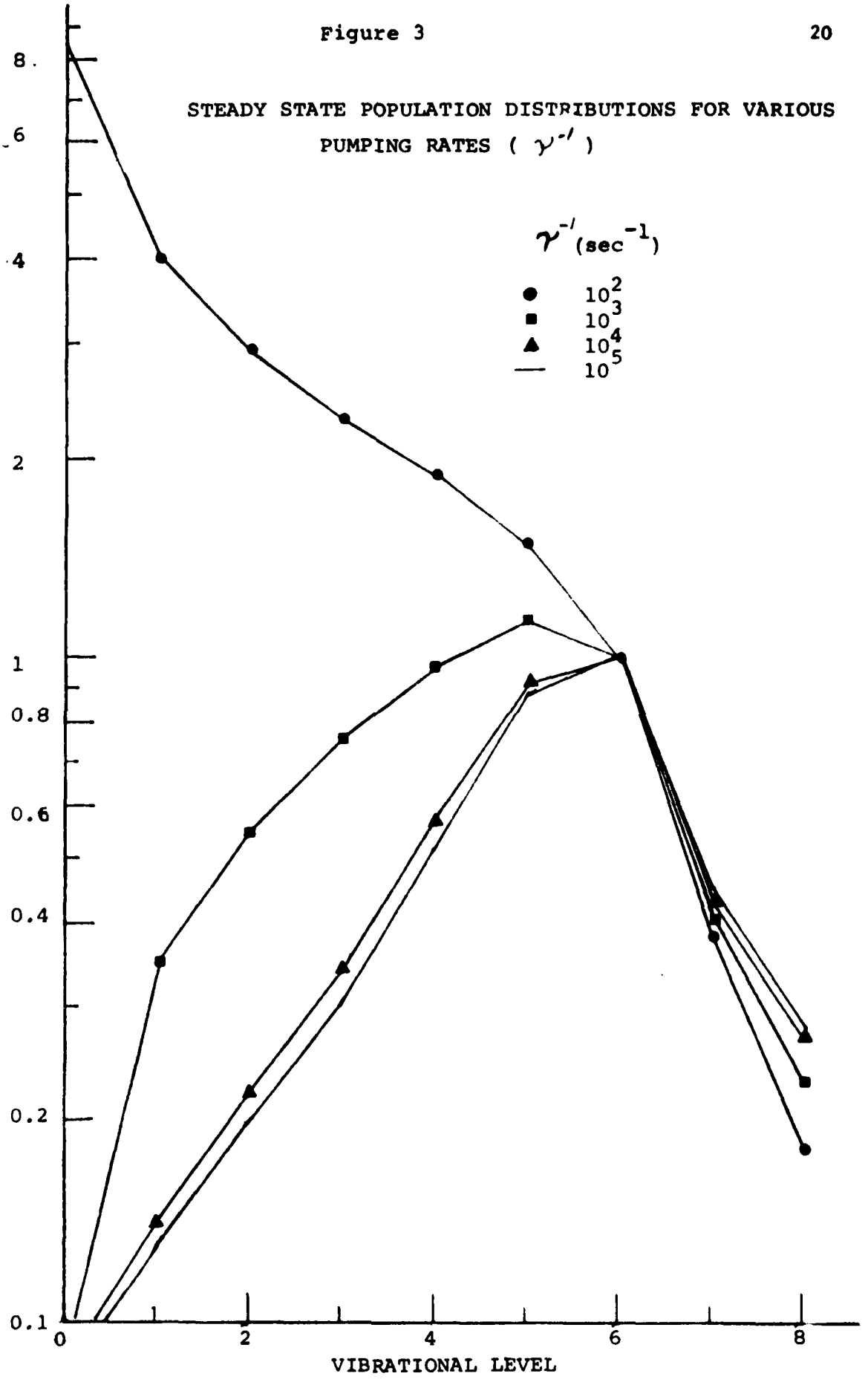

Figure 4

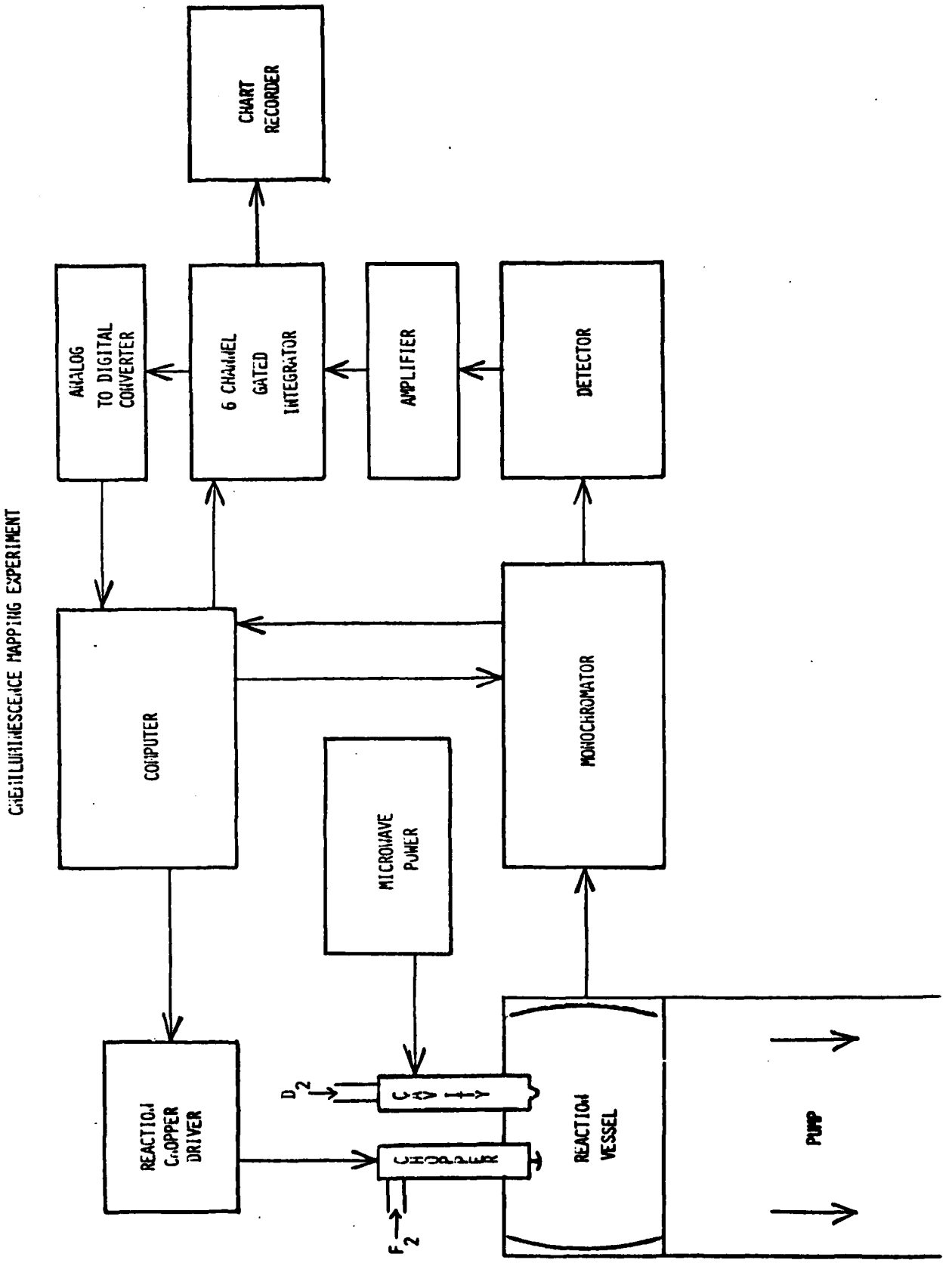
CHEMILUMINESCENCE MAPPING EXPERIMENT
CHART RECORDER
ANALOG TO DIGITAL CONVERTER
6 CHANNEL GATED INTEGRATOR
AMPLIFIER
DETECTOR
COMPUTER
MONOCHROMATOR
MICROWAVE POWER
REACTION CHOPPER DRIVER
D_2
CAVITY
CHOPPER
F_2
REACTION VESSEL
PUMP

Figure 5

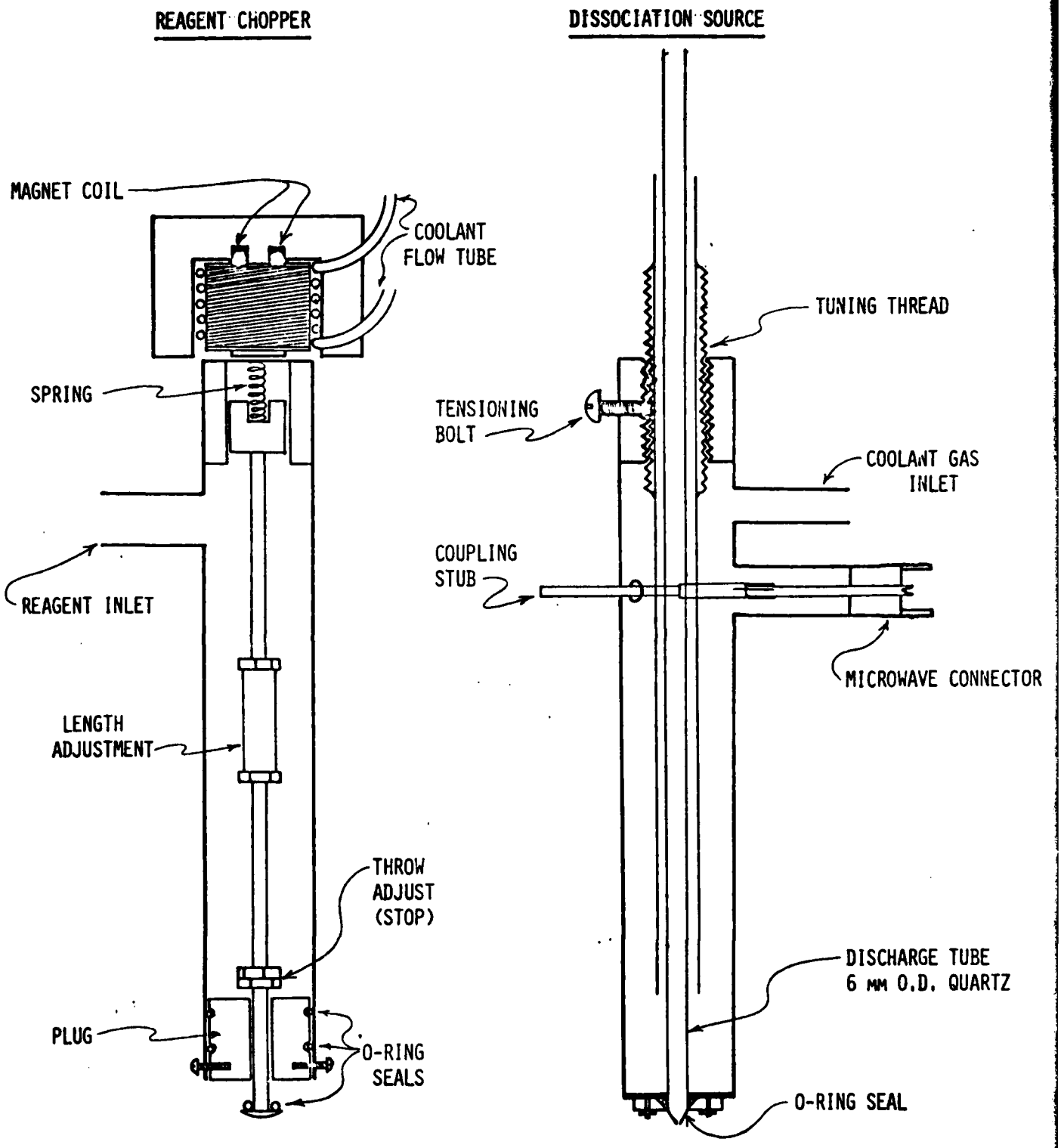
REAGENT CHOPPER
DISSOCIATION SOURCE
MAGNET COIL
COOLANT FLOW TUBE
SPRING
REAGENT INLET
LENGTH ADJUSTMENT
THROW ADJUST (STOP)
PLUG
O-RING SEALS
TUNING THREAD
TENSIONING BOLT
COOLANT GAS INLET
COUPLING STUB
MICROWAVE CONNECTOR
DISCHARGE TUBE 6 mm O.D. QUARTZ
O-RING SEAL

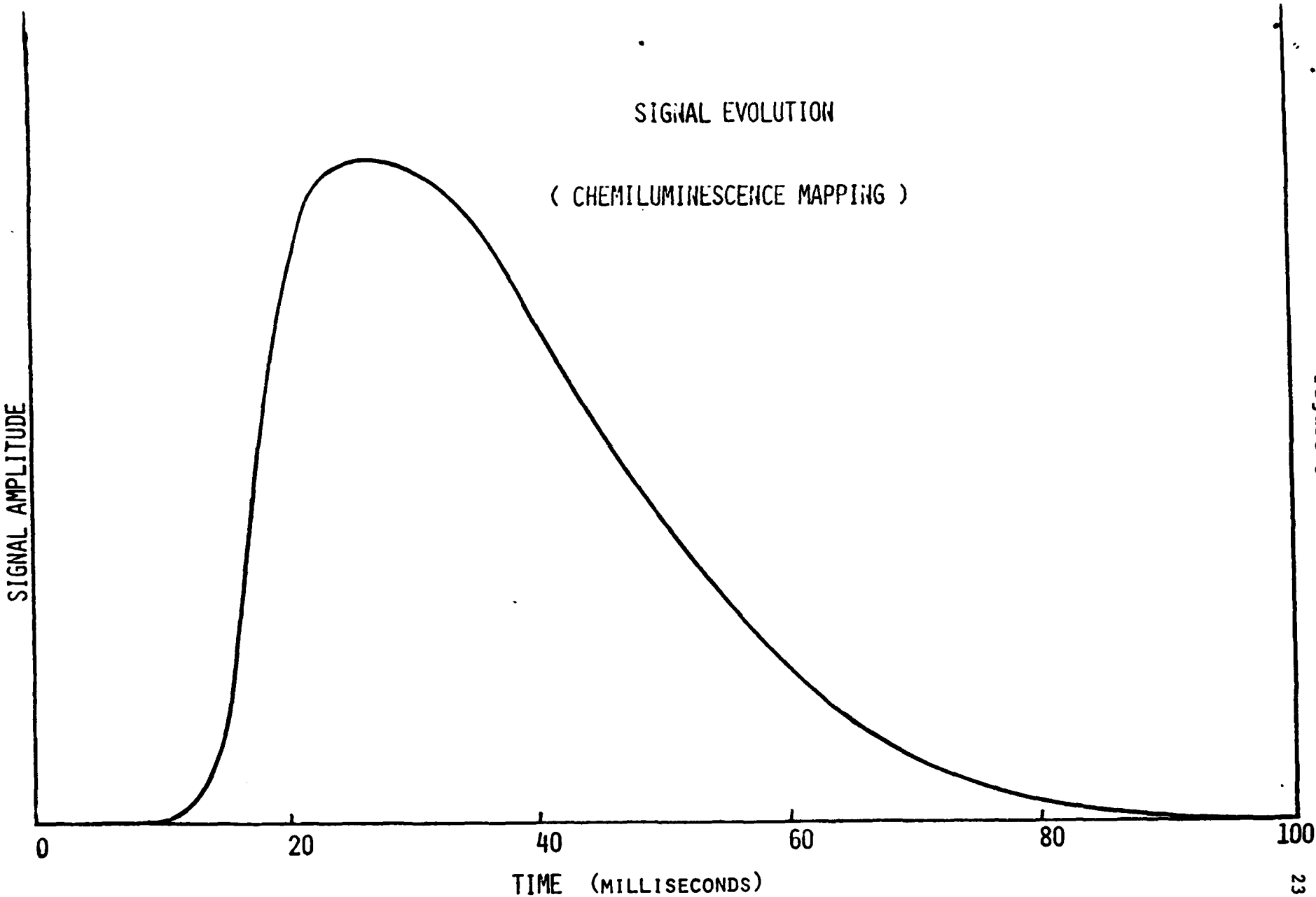
SIGNAL EVOLUTION
(CHEMILUMINESCENCE MAPPING)
SIGNAL AMPLITUDE
0
20
40
60
80
100
TIME (MILLISECONDS)

Figure 6.

Figure 7.

RELATIVE POPULATION vs INTEGRATOR CHANNEL

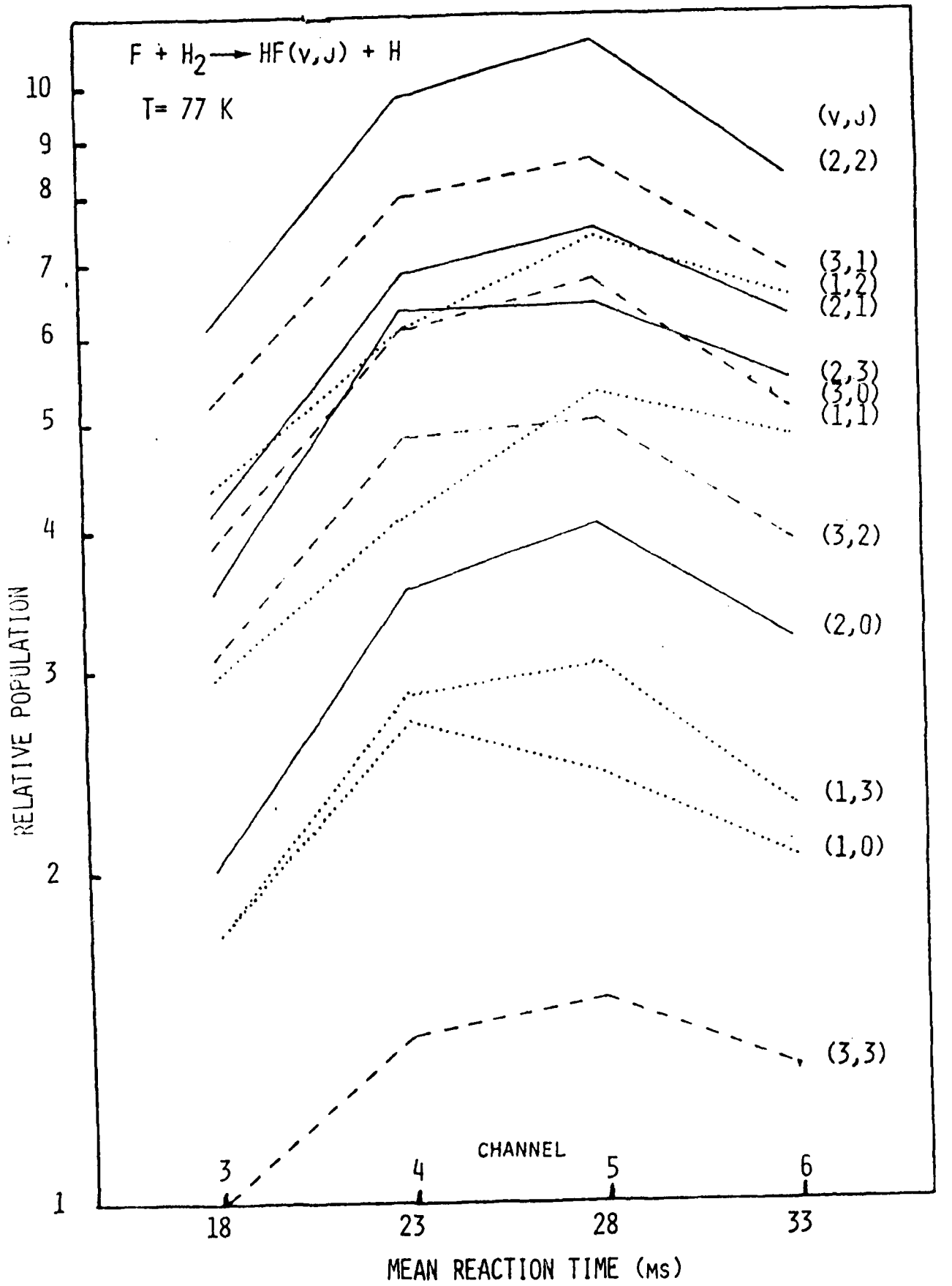

ROTATIONAL DISTRIBUTIONS FOR V= FROM D + F_2 REACTION

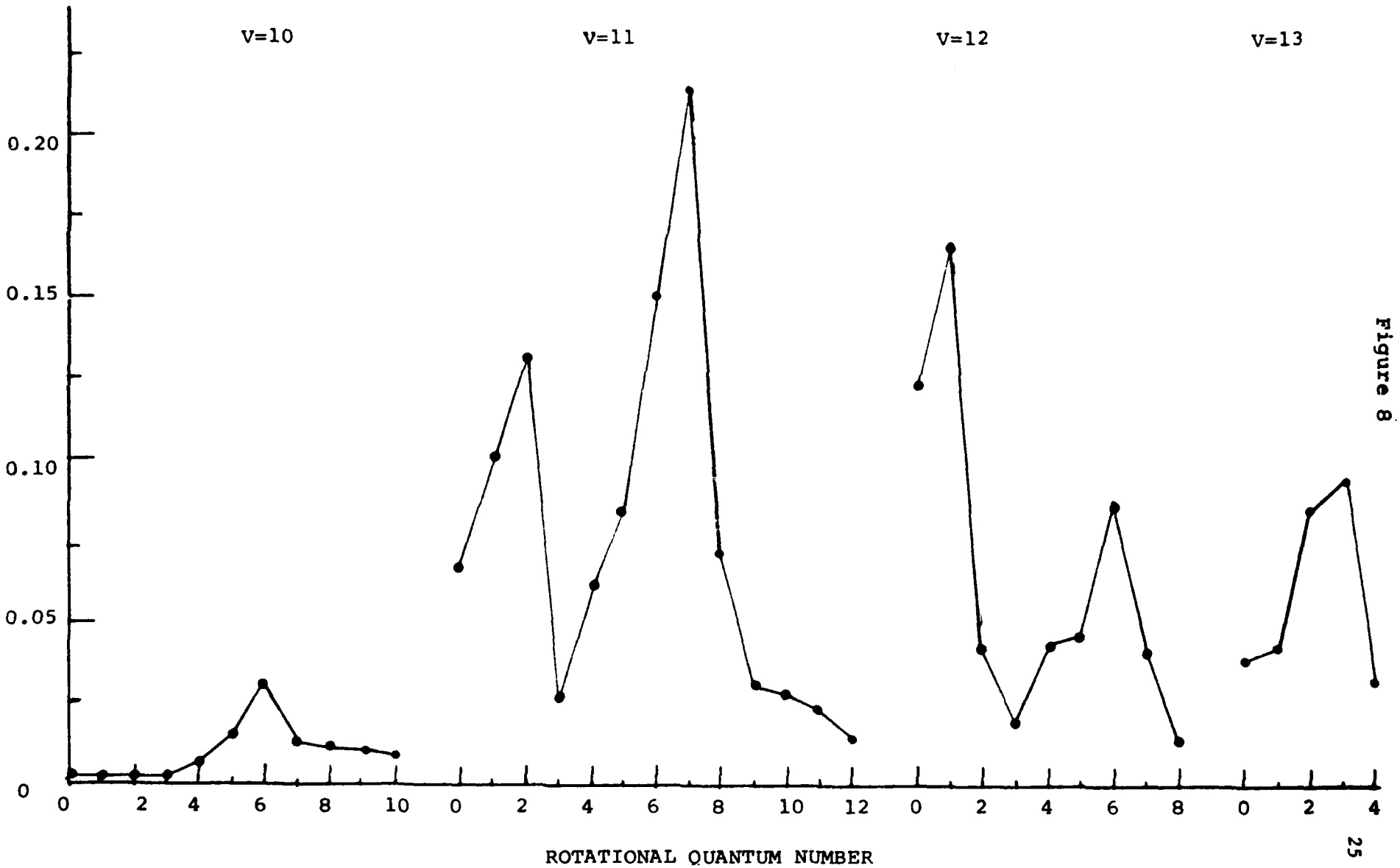

Figure 8

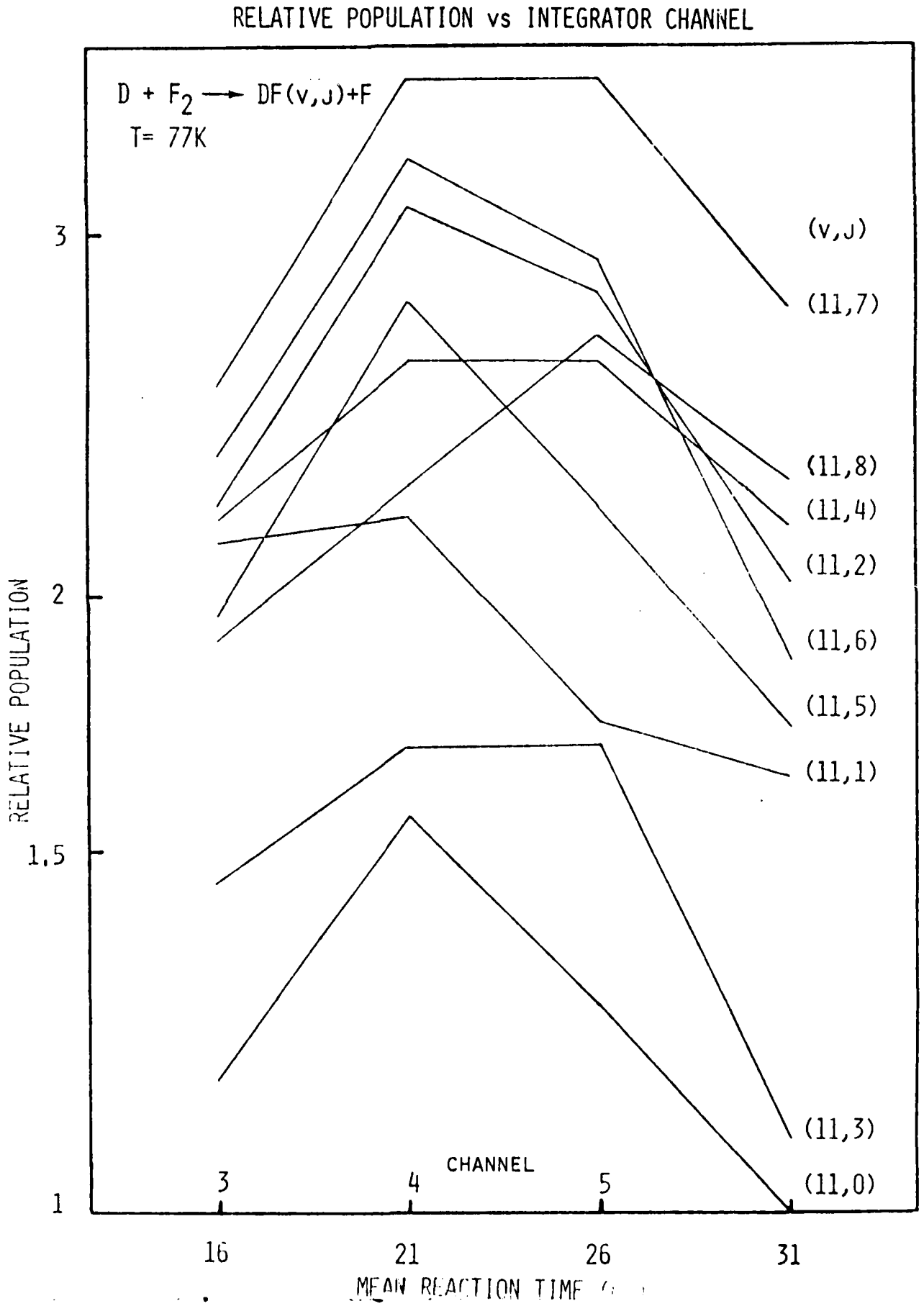
RELATIVE POPULATION vs INTEGRATOR CHANNEL
D + F2 → DF(v,J)+F
T= 77K
(v,J)
(11,7)
(11,8)
(11,4)
(11,2)
(11,6)
(11,5)
(11,1)
(11,3)
(11,0)
RELATIVE POPULATION
3
2
1.5
1
CHANNEL
3
4
5
16
21
26
31
MEAN REACTION TIME

Figure 10

RADIATIVE RATE CONSTANTS INCLUDING TRANSITIONS UP TO ΔV